GEOLOGICA CARPATHICA, APRIL 2015, 66, 2, 83–97 doi: 10.1515/geoca-2015-0012

Provenance of the Permian Malužiná Formation sandstones (Malé Karpaty Mountains, Western Carpathians): evidence of garnet and tourmaline mineral chemistry

MAREK VĎAČNÝ[1] and PETER BAČÍK[2]

[1]Geological Institute, Slovak Academy of Sciences, Branch: Ďumbierska 1, 974 01 Banská Bystrica, Slovak Republic; vdacny@savbb.sk
[2]Comenius University in Bratislava, Faculty of Natural Sciences, Department of Mineralogy and Petrology, Mlynská dolina G, 842 15 Bratislava, Slovak Republic; bacikp@fns.uniba.sk

(Manuscript received September 9, 2014; accepted in revised form March 12, 2015)

Abstract: The chemistry of detrital garnets (almandine; spessartine-, grossular-, and pyrope-rich almandine; andradite) and mostly dravitic tourmalines from three sandstone samples of the Permian Malužiná Formation in the northern part of the Malé Karpaty Mts (Western Carpathians, SW Slovakia) reveals a great variability of potential source rocks. They comprise (1) low-grade regionally metamorphosed rocks (metacherts, blue schists, metapelites and metapsammites), (2) contact-thermal metamorphic calcareous rocks (skarns or rodingites), (3) garnet-bearing mica schists and gneisses resulting from the regional metamorphism of argillaceous sediments, (4) amphibolites and metabasic sub-ophiolitic rocks, (5) granulites, (6) Li-poor granites and their associated pegmatites and aplites as well as (7) rhyolites. Consequently, the post-Variscan, rift-related sedimentary basin of the Malužiná Formation originated in the vicinity of a low- to high-grade crystalline basement with granitic rocks. Such lithological types of metamorphic and magmatic rocks are characteristic for the Variscan terranes of the Central Western Carpathians (Tatricum and Veporicum Superunits).

Key words: Permian, Western Carpathians, detrital heavy minerals, Hronicum Unit.

Introduction

With the advent of sophisticated microanalytical techniques in the last decades, many heavy mineral provenance studies became geochemically oriented. A large range of detrital heavy mineral species, including garnets, chromian spinel, tourmalines, amphiboles, pyroxenes, zircon, apatites, ilmenite and rutile, has been subjected to geochemical analyses (for review, see Mange & Morton 2007). Among them, garnet geochemistry has turned to be the most widely used mineral-chemical tool for determination and discrimination of sediment provenance because garnet is a common member of many heavy mineral assemblages and is a relatively stable mineral under both weathering and burial diagenetic conditions (Morton & Hallsworth 1999, 2007). Moreover, the garnets show a wide range in major element compositions depending on the lithology of the parent rocks. Likewise, chemical compositions of tourmaline-supergroup minerals vary in a wide range, which also makes them ideal minerals for geochemical discrimination of provenance. Henry & Guidotti (1985) and Henry & Dutrow (1992) demonstrated that tourmaline geochemistry reflects very well the local environment in which the mineral developed. Specifically, they showed that the Al–Fe_{total}–Mg and the Ca–Fe_{total}–Mg ternary diagram enable us to distinguish tourmalines from a variety of rock types. This important finding enhanced the application of tourmaline geochemistry in provenance studies (e.g. von Eynatten & Gaupp 1999; Nascimento et al. 2007; Morton et al. 2011, 2013; Jian et al. 2013).

The provenance of the Permian sandstones from the Malužiná Formation in the Malé Karpaty Mts (Hronicum Unit, Western Carpathians, Slovakia) has already been investigated several times. However, previous provenance studies on the Malužiná Formation sandstones concentrated mainly on either petrography of major framework grains and modal analysis of detrital framework components (Vďačný 2013) or on bulk rock geochemistry (Vďačný et al. 2013). Both modal and bulk rock analyses, however, produce only an overall composition of the source rocks and cannot determine if within-sample provenance mixing took place (c.f. Cawood 1991). On the other hand, the mineral chemistry of detrital heavy minerals documents not only within-sample provenance mixing but also provides more detailed information on source rock characteristics (Asiedu et al. 2000). In addition, data obtained from mineral chemistry of derived detrital constituents can be directly compared with those from potential source terranes.

Accordingly, the main objective of this study was to obtain more specific information on the lithology of potential parent source rocks for the Malužiná Formation sandstones from the Malé Karpaty Mts by examining the chemical composition of the detrital garnets and tourmalines. Moreover, this study brings a more detailed picture about the paleogeographical setting of the Malužiná Formation sandstones.

General geology

For the present study, we collected sandstone samples from the Malužiná Formation of the Ipoltica Group, situated in the Hronicum Unit in the northern part of the Malé Kar-

paty Mts (Fig. 1). The type profile of the Malužiná Formation is located in the Ipoltica valley and is completed by data from the Malužiná valley in the Nízke Tatry Mts (Vozárová & Vozár 1981). The Malužiná Formation attains regional extent in the basal part of the Hronicum Unit; its thickness attains up to 2200 m, as calculated from some outcrops in the Nízke Tatry Mts and from borehole data in the basement of the Middle Slovakian neovolcanic area (Vozárová & Vozár 1981, 1988). The lower boundary towards the lower Nižná Boca Formation (a part of the Ipoltica Group) is lithological. The upper boundary is again lithological towards the sediments of the Lower Triassic age situated above the Malužiná Formation concordantly without sedimentary interruption.

As concerns the lithology (Fig. 2), the main features of the Malužiná Formation include: (1) an internal arrangement into three megacycles; (2) presence of synchronous volcanite layers and bodies of basic to intermediate composition and of slight to pronounced tholeiitic chemistry (Vozár 1977, 1997; Dostal et al. 2003) in the first and third megacycles; and (3) a variegated colour of sediments ranging from red, brown, violet, grey to whitish-grey (Vozárová & Vozár 1981, 1988).

In the Malužiná Formation, the amount of coarse detrital constituents is higher when compared with the Nižná Boca Formation (Fig. 2). Coarse sandstone to conglomerate layers constitute the basal parts of all three megacycles. Single beds are well developed with graded bedding at the base, but planar to laminar bedding in the upper parts.

The middle portions of single megacycles reveal a cyclical internal structure in which medium- to coarse-grained clastics predominate. Commonly, single cycles are asymmetrical and composed of sandstone, aleurolite to aleuropelite. Shale to aleurolite intraclasts occur here frequently (Vozárová & Vozár 1981).

The upper portions of megacycles have again cyclical internal structures mainly made of fine sediments. Laminar to horizontal stratification prevails in aleurite to aleuropelite rocks. Layers with carbonate concretions together with gypsum to anhydrite lenses (Drnzík 1969; Novotný & Badár 1971) occur mostly in the upper parts of the first and second megacycles (Fig. 2). Organic hieroglyphs were observed there as well.

The Malužiná Formation ranges from the Early to the Late Permian age (Planderová 1973; Planderová & Vozárová 1982). This was also corroborated by the $^{206}Pb/^{238}U$ and $^{207}Pb/^{235}U$ dating. An age of 263 ± 11 Ma was documented from uranium-rich layers of the upper part of the second megacycle (Rojkovič 1997). Clastic micas from sandstones of the second megacycle, which were analysed by the

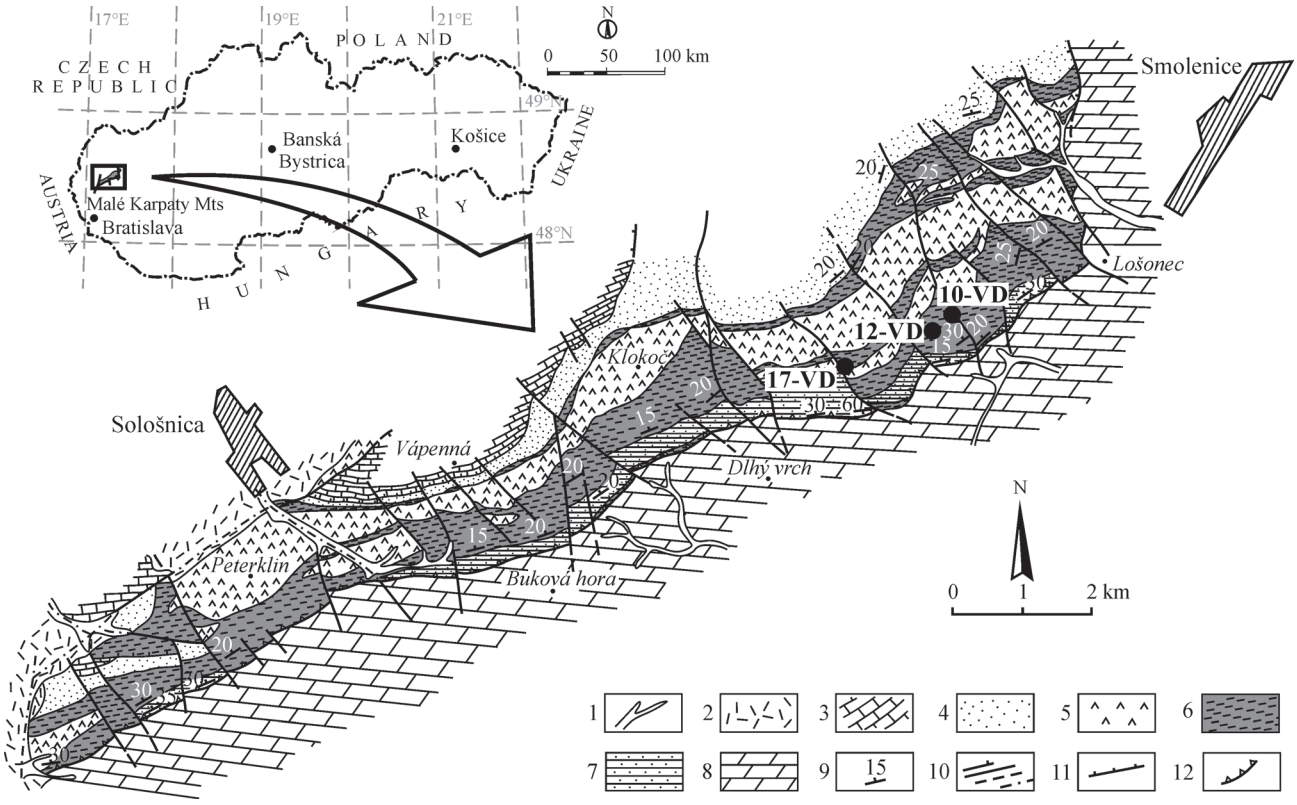

Fig. 1. Schematic geological map of the Upper Paleozoic rocks of the Hronicum Unit in the Malé Karpaty Mts (after Vozárová & Vozár 1988). Sampling localities of sandstone samples collected south-west of Smolenice are indicated. **Explanations:** 1 — Quaternary sediments, 2 — Tertiary sediments. **Hronicum Unit–Šturec Nappe:** 3 — Middle and Upper Triassic — carbonates, undivided, 4 — Lower Triassic — quartz sandstones, shales, 5 — Late Paleozoic–Permian — andesites, basalts, and volcanoclastics (Malužiná Formation), 6 — Late Paleozoic–Permian — conglomerates, sandstones, shales with volcanigenic material admixture (Malužiná Formation), 7 — Late Paleozoic–Stephanian — grey conglomerates, sandstones, shales (Nižná Boca Formation). **Krížna Nappe:** 8 — Mesozoic, undivided. **Others:** 9 — foliation cleavage, 10 — faults, 11 — overthrusts, 12 — overthrust line of nappes.

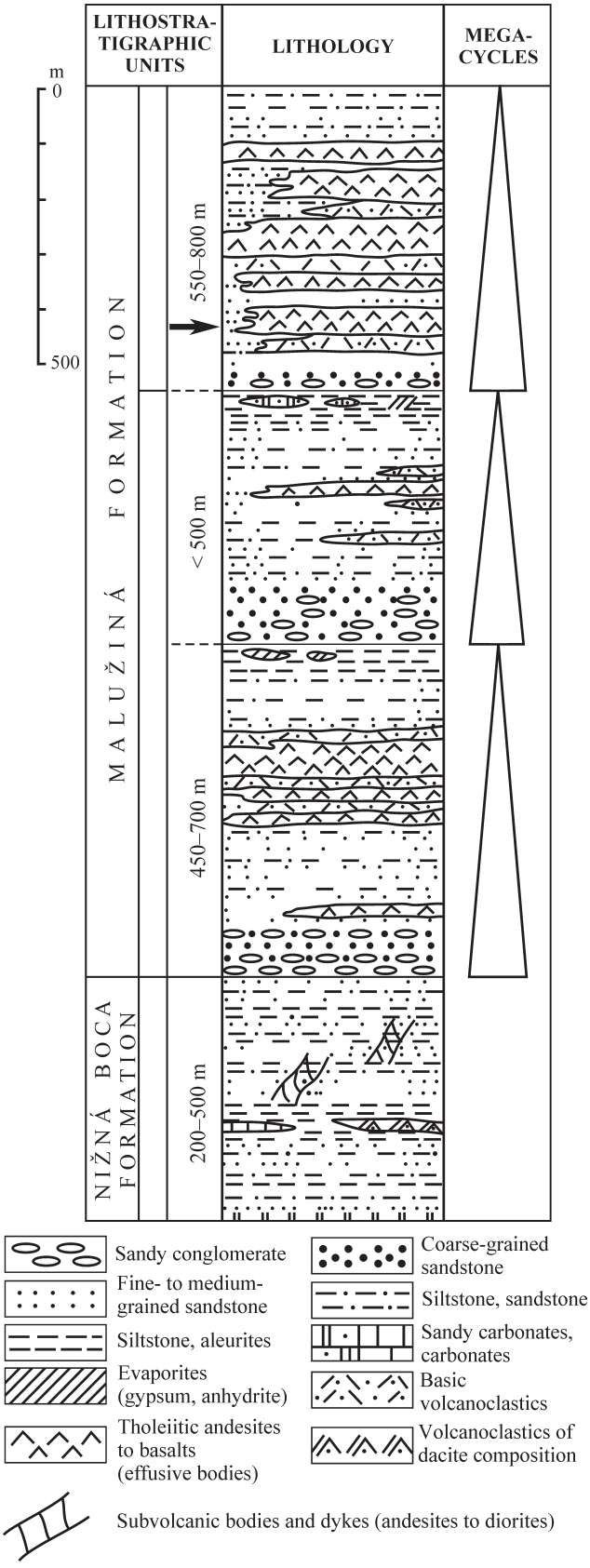

Fig. 2. Schematic lithostratigraphical subdivision of the Ipoltica Group (Vozárová & Vozár 1981) with approximate indication of the places of sampling (marked by an arrow).

$^{40}Ar/^{39}Ar$ method, revealed 342 ± 3 Ma as the age of cooling of the source area (Vozárová et al. 2005).

The sedimentary environment was of a deltaic to lacustrine character (Vozárová & Vozár 1981, 1988; Vozárová et al. 2009). Considerable size of the water reservoir with higher salinity is indicated by the preserved sedimentary structures, overwhelming turbidite sandstone layers, organic hieroglyphs and chemogenous layers. Synsedimentary tectonic activity concentrated to movements along the subvertical faults confining the sedimentary domains. Further, this activity was connected with rifting movements in the basinal centers, which is reflected by the megacyclic internal structure of the Malužiná Formation with mostly coarse detrital sediments in the basal portions of single megacycles as well as by the repeated extrusions that produced volcanic layers (Vozárová & Vozár 1981, 1988). In the palinspastic picture of Variscan basins of the Western Carpathians, the Upper Paleozoic sediments of the Hronicum Unit reveal typical features of basins created by the rifting tectonic regime along the southern periphery of the Variscan orogenic belt (Vozárová & Vozár 1981, 1988).

Petrographic composition of the sampled sandstones

Detrital garnets and tourmalines were studied in three sandstone samples. All came from the third megacycle of the Malužiná Formation (Fig. 2). These three sandstone samples have a low primary matrix content, spanning the range of 0.4–5.6 %. The dominant detrital components are quartz grains, whereby monocrystalline (29.8–53.2 %) prevails over polycrystalline (8.6–13.6 %) quartz. Thus, the ratio of monocrystalline to polycrystalline quartz varies from 2.2 to 6.2. The fragments of potassium feldspars (K) and plagioclases (P) are in similar amounts, causing the K/P ratio to oscillate around 1 (K/P = 0.8–1.3). The content of clastic mica in the sandstones is negligible, ranging from 0 to 0.8 %. Likewise, the content of metamorphic rock fragments is comparatively uniform, varying only slightly from 2.6 to 3.2 %. On the other hand, the content of volcanic (0.2–16.2 %) and sedimentary (0.4–5.0 %) lithic fragments varies more distinctly.

The composition of heavy mineral assemblages is as follows: apatite (2.5–25.0 %), biotite (3.2–17.5 %), garnet (13.7–15.9 %), hematite, ilmenite and magnetite (4.4–67.3 %), titanite (5.3–26.3 %), tourmaline (3.2–24.8 %), and zircon (2.8–8.0 %). The zircon-tourmaline-rutile (ZTR) index (Hubert 1962) varies from 20.2 to 42.1 %. These comparatively low ZTR index values indicate mineralogical immaturity of the sampled sandstones.

Analytical techniques

In three sandstone samples 10-VD, 12-VD, and 17-VD, detrital garnet and tourmaline crystals were separated from heavy mineral concentrates obtained from crushed rock using standard procedures described by Mange & Maurer (1992). These procedures included sieving to obtain the

0.063–0.250 mm fraction, separation in heavy liquid (bromoform of $D = 2.8$ g/cm^3) and finally hand picking of individual grains. Acquired garnets and tourmalines were then mounted in epoxy resin, polished and coated with carbon for electron microprobe analysis (EMPA).

The EMPA was carried out using a Cameca SX-100 electron microprobe at the Department of Electron Microanalysis at the State Geological Institute of Dionýz Štúr in Bratislava (Slovak Republic). The apparatus is equipped with four wavelength-dispersive mode spectrometers. During the procedure an accelerating voltage of 15 kV, a beam current of 20 nA and a beam focussed to 5 μm were used. The following standards and measured lines were used: orthoclase (Si $K\alpha$, K $K\alpha$), TiO_2 (Ti $K\alpha$), Al_2O_3 (Al $K\alpha$), metallic Cr (Cr $K\alpha$), fayalite (Fe $K\alpha$), rhodonite (Mn $K\alpha$), metallic Ni (Ni $K\alpha$), forsterite (Mg $K\alpha$), wollastonite (Ca $K\alpha$), albite (Na $K\alpha$), LiF (F $K\alpha$), and NaCl (Cl $K\alpha$). Raw data were processed using the Quantiview software provided by Cameca and the PAP routine was used for data correction. A total of 45 garnets in three samples (10-VD, 12-VD, and 17-VD) and 29 tourmalines in two samples (10-VD and 12-VD) were analysed in this study using single-spots. One to three spots per grain were randomly placed in the grain core parts.

The garnet crystal-chemical formula calculation was based on 8 cations. The Fe^{2+}/Fe^{3+} proportion was calculated from the charge-balanced formula. The tourmaline crystal-chemical formulae were calculated on the basis of $15Y+Z+T$ cations, Fe^{2+}/Fe^{3+} proportion and $^{W}O^{2-}$ were obtained from the charge-balanced formula, OH was calculated as OH = 4–F–Cl–^{W}O apfu (atoms per formula unit), B = 3 apfu.

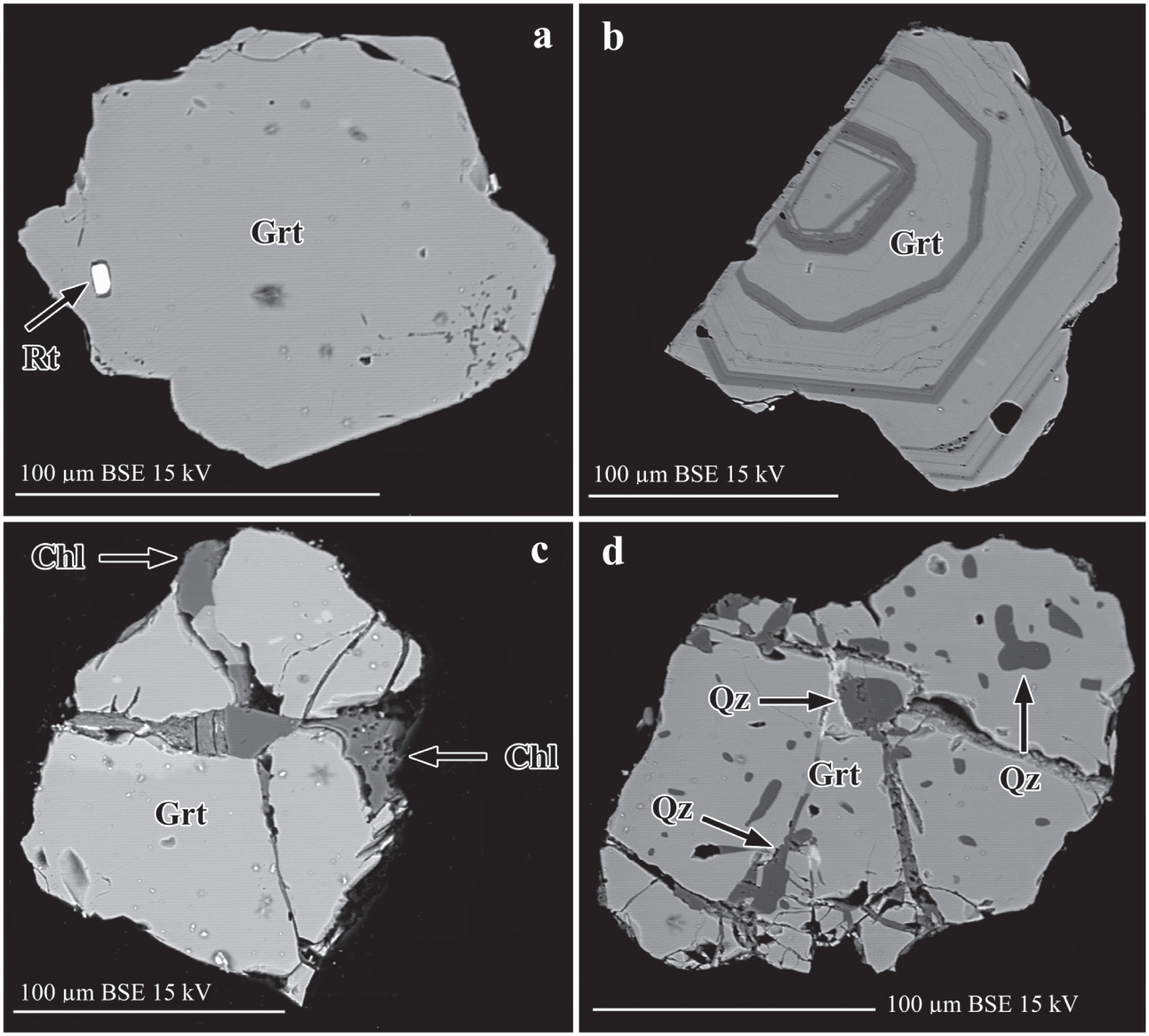

Fig. 3. Representative back-scattered electron (BSE) images of garnets (Grt) from the sandstone samples 12-VD and 17-VD. **a** — A grain with inclusion of rutile (Rt), **b** — A grain with thin regular dark zones, **c** — A split grain filled with chlorite (Chl), **d** — A grain with dark inclusions of quartz (Qz).

Results

Chemical composition and features of garnets

Garnets in the sandstone samples studied are subhedral to anhedral, up to 200 μm in size (Fig. 3). They do not display any inherited cores or overgrowth marginal zones. However, some of them contain inclusions of quartz, rutile, apatite, and muscovite.

The majority of garnets have almandine composition, with a predominance of the spessartine component only in a single garnet grain in the 12-VD sample and two crystals in the 17-VD showing andradite composition (Table 1, Fig. 4). The dominant almandine component varies between 62 and 68 mol % in the 10-VD sample, 37 and 80 mol % in the 12-VD sample and attains 52 to 74 mol % in the 17-VD sample. If we exclude rare andradite compositions, spessartine is usually the second most abundant component in the majority of the studied garnet grains. It achieves 22 mol % in 10-VD, 39 mol % in 12-VD, and 30 mol % in 17-VD. The grossular component is relatively abundant in 12-VD (up to 26 mol %) and 17-VD (≤32 mol %), while it is very low in 10-VD (≤1.9 mol %). The pyrope component is mostly enriched in the 12-VD sam-

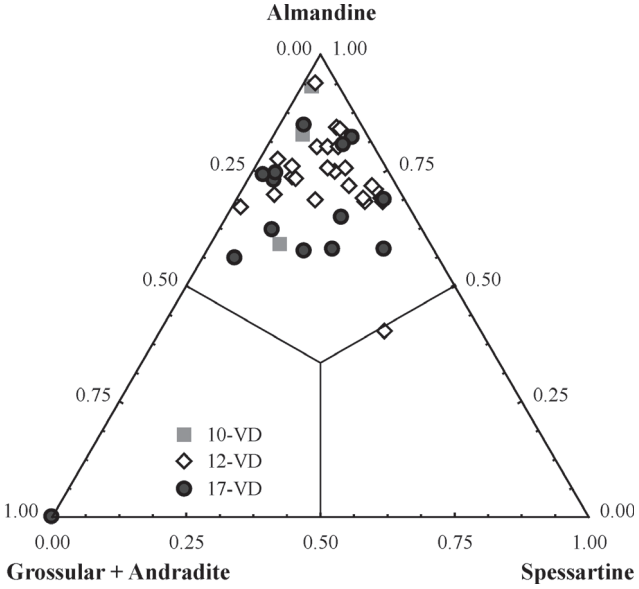

Fig. 4. Classification diagram of garnets (n = 45) from the sandstones studied based on the end-member component proportions.

Table 1: Representative electron microprobe analyses of detrital garnets from the Malužiná Formation sandstones.

Sample	10-VD	10-VD	12-VD	12-VD	12-VD	17-VD	17-VD	17-VD
Analysis no.	7	9	6	19	29	5	6	14
SiO_2	36.38	36.72	37.48	38.92	37.09	36.10	37.43	34.14
TiO_2	0.03	0.03	0.02	0.08	0.11	0.03	0.19	0.00
Al_2O_3	21.08	21.02	21.42	22.50	20.97	20.97	21.33	0.00
Cr_2O_3	0.00	0.03	0.03	0.17	0.03	0.00	0.01	0.00
Fe_2O_3	2.50	2.24	0.91	1.63	1.26	2.41	0.76	32.08
FeO	26.93	29.58	35.21	20.39	27.48	26.75	32.99	0.00
MnO	9.63	5.04	0.74	0.56	10.75	11.19	1.78	0.44
MgO	3.19	3.69	3.73	8.68	2.40	1.93	3.18	0.00
NiO	0.00	0.02	0.00	0.00	0.00	0.00	0.00	0.00
CaO	0.91	1.97	1.55	7.95	1.33	1.12	3.31	32.75
Na_2O	0.00	0.03	0.05	0.00	0.02	0.05	0.05	0.03
Total	100.68	100.36	101.14	100.89	101.43	100.55	101.04	99.44
Si^{4+}	2.923	2.940	2.973	2.942	2.968	2.927	2.971	2.911
Al^{3+}	0.077	0.060	0.027	0.058	0.032	0.073	0.029	0.000
Fe^{3+}	0.000	0.000	0.000	0.000	0.000	0.000	0.000	0.089
ΣZ	3.000	3.000	3.000	3.000	3.000	3.000	3.000	3.000
Ti^{4+}	0.002	0.002	0.001	0.005	0.007	0.002	0.011	0.000
Al^{3+}	1.920	1.924	1.976	1.946	1.945	1.930	1.967	0.000
Cr^{3+}	0.000	0.002	0.002	0.010	0.002	0.000	0.000	0.000
Fe^{3+}	0.078	0.073	0.021	0.039	0.047	0.068	0.021	1.970
Mn^{2+}	0.000	0.000	0.000	0.000	0.000	0.000	0.000	0.030
Σ*Y*	2.000	2.000	2.000	2.000	2.000	2.000	2.000	2.000
Fe^{3+}	0.073	0.062	0.033	0.053	0.029	0.079	0.025	0.000
Fe^{2+}	1.810	1.981	2.336	1.289	1.839	1.814	2.190	0.000
Mn^{2+}	0.656	0.342	0.050	0.036	0.729	0.768	0.119	0.001
Mg^{2+}	0.382	0.441	0.441	0.978	0.286	0.234	0.376	0.001
Ni^{2+}	0.000	0.001	0.000	0.000	0.000	0.000	0.000	0.000
Ca^{2+}	0.079	0.169	0.132	0.644	0.114	0.098	0.282	2.993
Na^{+}	0.000	0.004	0.008	0.000	0.003	0.007	0.008	0.005
Σ*X*	3.000	3.000	3.000	3.000	3.000	3.000	3.000	3.000
Pyrope	12.57	14.71	14.74	32.62	9.55	7.80	12.57	0.02
Spessartine	21.59	11.42	1.66	1.19	24.31	25.65	3.99	0.05
Almandine	61.85	68.10	79.12	44.38	61.83	63.02	73.34	0.00
Andradite	3.83	3.63	1.04	1.97	2.36	3.39	1.05	98.66
Uvarovite	0.00	0.08	0.08	0.52	0.08	0.00	0.02	0.00
Schorlomite	0.16	0.12	0.07	0.35	0.50	0.15	0.69	0.00
Grossular	0.00	1.93	3.29	18.97	1.37	0.00	8.34	1.27
Σ	100.00	100.00	100.00	100.00	100.00	100.00	100.00	100.00

Table 2: Representative electron microprobe analyses of detrital tourmalines from the Malužiná Formation sandstones.

Sample	10-VD	10-VD	10-VD	10-VD	12-VD	12-VD	12-VD	12-VD
Analysis no.	1	2	5	13	4	18	33	37
SiO_2	36.15	36.63	35.97	35.78	36.87	37.02	37.26	36.52
TiO_2	0.83	0.53	0.75	0.45	0.47	0.70	0.69	0.14
B_2O_3*	10.57	10.55	10.47	10.27	10.55	10.69	10.67	10.61
Al_2O_3	32.86	32.09	33.47	29.02	32.24	32.51	32.31	32.12
Cr_2O_3	0.08	0.00	0.02	0.01	0.02	0.02	0.09	0.00
Fe_2O_3	0.00	0.00	0.00	0.31	0.00	0.00	0.00	0.00
FeO	4.22	5.96	6.77	12.67	8.89	6.20	4.49	7.61
MnO	0.01	0.00	0.03	0.00	0.07	0.00	0.00	0.00
MgO	8.13	7.51	5.79	4.99	5.56	7.49	8.30	7.20
NiO	0.00	0.01	0.00	0.00	0.02	0.01	0.03	0.00
CaO	1.00	0.47	0.47	0.22	0.26	0.64	1.31	0.12
Na_2O	1.98	2.25	1.86	2.62	2.02	2.19	2.00	2.62
K_2O	0.02	0.02	0.02	0.02	0.02	0.01	0.02	0.02
H_2O*	3.22	3.35	3.19	3.54	3.39	3.35	3.11	3.58
F	0.00	0.00	0.00	0.00	0.00	0.00	0.00	0.00
Cl	0.01	0.00	0.01	0.01	0.01	0.01	0.00	0.02
O=F	0.00	0.00	0.00	0.00	0.00	0.00	0.00	0.00
O=Cl	0.00	0.00	0.00	0.00	0.00	0.00	0.00	0.00
Total	99.08	99.35	98.83	99.91	100.38	100.84	100.29	100.57
Si	5.944	6.036	5.974	6.057	6.075	6.021	6.069	5.982
Al	0.056	0.000	0.026	0.000	0.000	0.000	0.000	0.018
Σ*T*	6.000	6.036	6.000	6.057	6.075	6.021	6.069	6.000
B	3.000	3.000	3.000	3.000	3.000	3.000	3.000	3.000
Al	5.990	6.000	5.997	5.790	5.998	5.997	5.989	6.000
Cr	0.010	0.000	0.003	0.001	0.002	0.003	0.011	0.000
Mg	0.000	0.000	0.000	0.209	0.000	0.000	0.000	0.000
Σ*Z*	6.000	6.000	6.000	6.000	6.000	6.000	6.000	6.000
Ti	0.102	0.066	0.094	0.057	0.059	0.085	0.085	0.017
Al	0.323	0.231	0.529	0.000	0.264	0.234	0.215	0.183
Fe^{3+}	0.000	0.000	0.000	0.040	0.000	0.000	0.000	0.000
Fe^{2+}	0.580	0.821	0.940	1.794	1.225	0.843	0.612	1.042
Mn	0.002	0.000	0.005	0.000	0.009	0.001	0.000	0.000
Mg	1.992	1.845	1.433	1.051	1.365	1.815	2.016	1.757
Ni	0.000	0.001	0.000	0.001	0.003	0.001	0.004	0.000
Σ*Y*	3.000	2.964	3.000	2.943	2.925	2.979	2.931	3.000
Ca	0.177	0.083	0.084	0.039	0.046	0.111	0.229	0.022
Na	0.633	0.717	0.600	0.859	0.645	0.691	0.633	0.833
K	0.004	0.004	0.003	0.004	0.003	0.002	0.004	0.005
Σ*X*	0.813	0.805	0.688	0.902	0.695	0.804	0.866	0.860
$^{X}\square$	0.187	0.195	0.312	0.098	0.305	0.196	0.134	0.140
F	0.000	0.000	0.000	0.000	0.000	0.000	0.000	0.000
Cl	0.002	0.000	0.003	0.002	0.003	0.001	0.000	0.005
O	0.461	0.323	0.462	0.000	0.272	0.361	0.618	0.081
OH	3.537	3.677	3.535	3.998	3.725	3.638	3.382	3.914
Σ*V*+*W*	4.000	4.000	4.000	4.000	4.000	4.000	4.000	4.000
Σcations	18.813	18.805	18.688	18.902	18.695	18.804	18.866	18.860
ΣAl	6.369	6.231	6.552	5.790	6.261	6.231	6.204	6.201
Mg/Fe	3.433	2.248	1.524	0.703	1.114	2.152	3.292	1.686
Na/Ca	3.583	8.626	7.139	21.887	14.033	6.209	2.762	38.056

*OH = 4–F–Cl–^{W}O apfu, B = 3 apfu.

ple in which it exhibits a range of 5.8 to 33 mol %. Garnets in the 10-VD sample have a medium content of pyrope component between 9.4 and 15 mol %, whereas in almandine crystals of the 17-VD sample, the pyrope constituent ranges between 3.6 and 13 mol %. The content of andradite end-member is typically low (≤4 mol %) with an exception of andradite-dominant grains in the 17-VD sample. Moreover, it reaches up to 6.2 mol % in 10-VD and 12-VD and is enriched only in a single almandine grain in the 17-VD sample having 19 mol %, although it usually does not exceed 4 mol % in this sample. The proportion of other components, such as uvarovite and schorlomite, is lower than 0.5 mol %.

The chemical composition of garnets is controlled by substitutions of cations in the *X* site. The most abundant Fe^{2+} cation is substituted mostly by Mn^{2+} but also by Ca^{2+} and Mg^{2+}. However, there is no general substitution trend present for all the analysed garnets. Aluminium is the vastly dominant cation in the *Y* site and is substituted by Fe^{3+} only insignificantly with an exception of andradite-enriched garnets. The andradite-dominant composition is the result of $CaFe^{3+}(Fe^{2+}, Mn, Mg)_{-1}Al_{-1}$ substitution.

To summarize, three major garnet groups and two minor garnet groups can be recognized from the chemical composition of the studied garnet grains. The major groups are al-

mandine, spessartine-rich almandine, and grossular-rich almandine garnets. They may be accompanied by two minor groups: pyrope-rich almandine and andradite garnets.

Chemical composition and features of tourmalines

Tourmalines in the sandstones form euhedral to subhedral prismatic crystals up to 200 μm in size (Fig. 5). Similarly to garnets, tourmalines also do not exhibit any inherited cores or overgrowth marginal zones.

Tourmalines from the 10-VD and 12-VD samples (Table 2) belong to the alkali group of tourmalines with dravitic composition (Fig. 6a,b). The atomic $Fe^{2+}/(Fe^{2+}+Mg)$ ratio is similar in both samples (Table 2) varying in the range of 0.22–0.34 and 0.23–0.47 in the 10-VD and 12-VD samples, respectively. Only one tourmaline crystal in the 10-VD sample shows schorlitic composition attaining the $Fe^{2+}/(Fe^{2+}+Mg)$ ratio of 0.63 (Fig. 6b). Tourmalines in the 10-VD sample are generally more alkali-deficient with the *X*-site vacancy proportion between 0.1 and 0.3 than in 12-VD with the *X*-site vacancy usually between 0.1 and 0.2, except for one analysis in a single tourmaline grain with 0.3 (Table 2, Figs. 6 and 7a). Likewise, 10-VD is enriched in Al with its content between 6.2 and 6.6 apfu with an exception of schorlitic tourmaline (5.8 apfu), while in 12-VD Al attains only up to 6.3 apfu (Table 2). The increase in vacancy and Al slightly shifts composition to the magnesio-foitite end-member (Fig. 7a). The composition of tourmaline is mainly controlled by the exchange of Fe^{2+} for Mg^{2+} (Fig. 7b). Moreover, both cations are mutually involved in $^{X}\square Al Na_{-1}(Mg, Fe^{2+})_{-1}$ (Fig. 7c) and $NaAlCa_{-1}(Mg, Fe^{2+})_{-1}$ (Fig. 7d) substitutions. However, the $^{X}\square Al Na_{-1}(Mg, Fe^{2+})_{-1}$ mechanism has a better correlation which suggests that the change in charge after the substitution of Al for Mg and Fe^{2+} is balanced preferentially by an increase in vacancy in the *X*-site rather than by the substitution of Na^{+} for Ca^{2+} which is typical for Al enriched compositions.

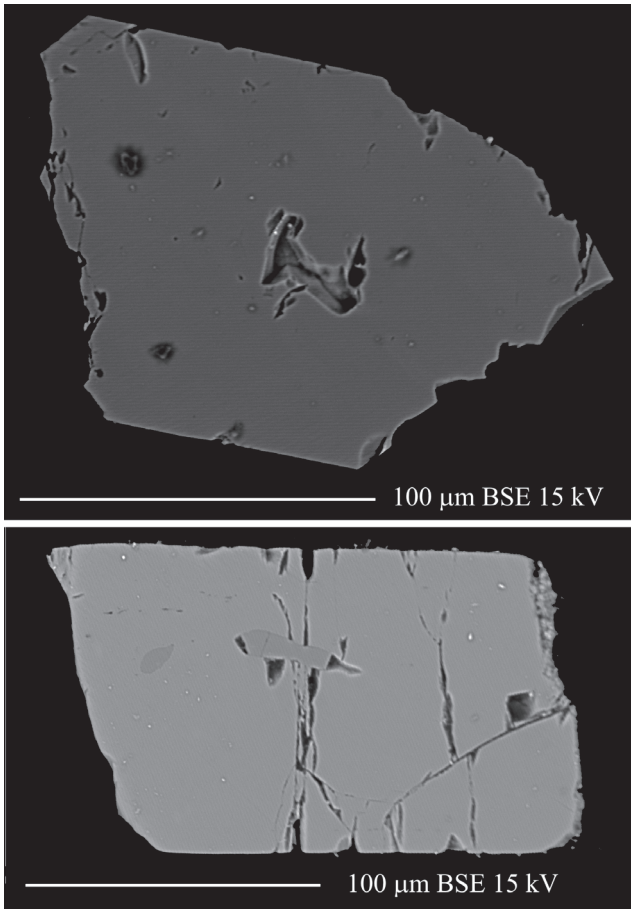

Fig. 5. Representative back-scattered electron (BSE) images to document the shape and size of two tourmaline grains from the sandstone sample 12-VD.

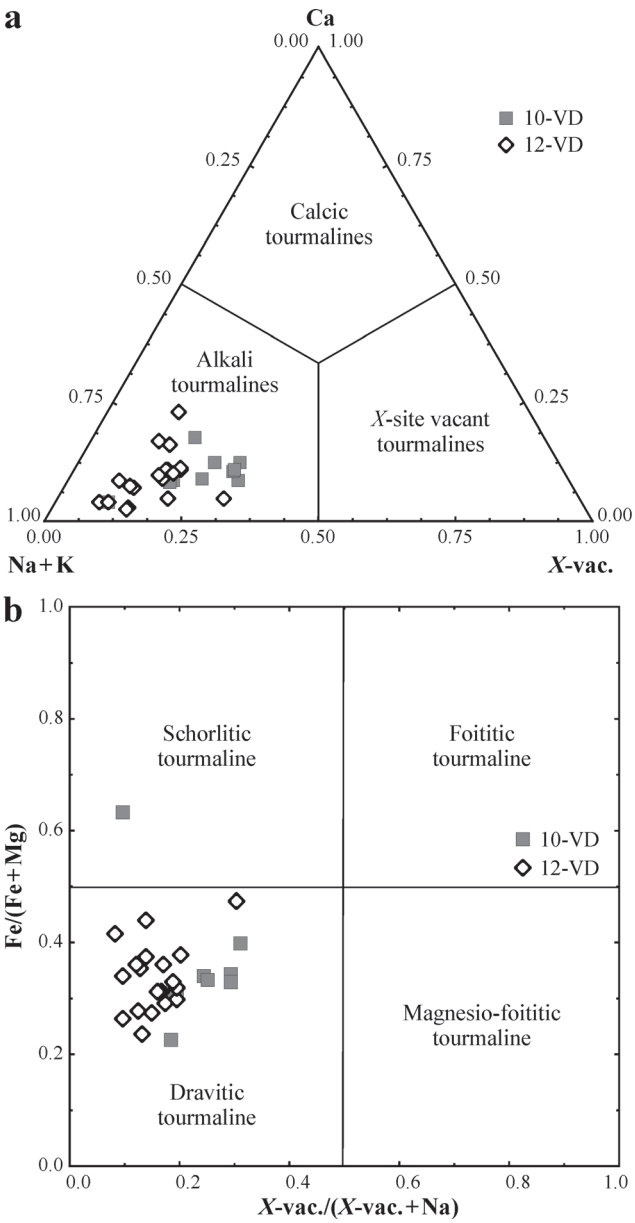

Fig. 6. Classification diagrams of tourmalines ($n=29$) from the sandstones. **a** — Classification into mineral groups based on the *X*-site occupancy (Hawthorne & Henry 1999), **b** — Classification into generalized mineral species based on the *X*-site vacancy and $Fe^{2+}/(Fe^{2+}+Mg)$ proportion (Henry et al. 2011).

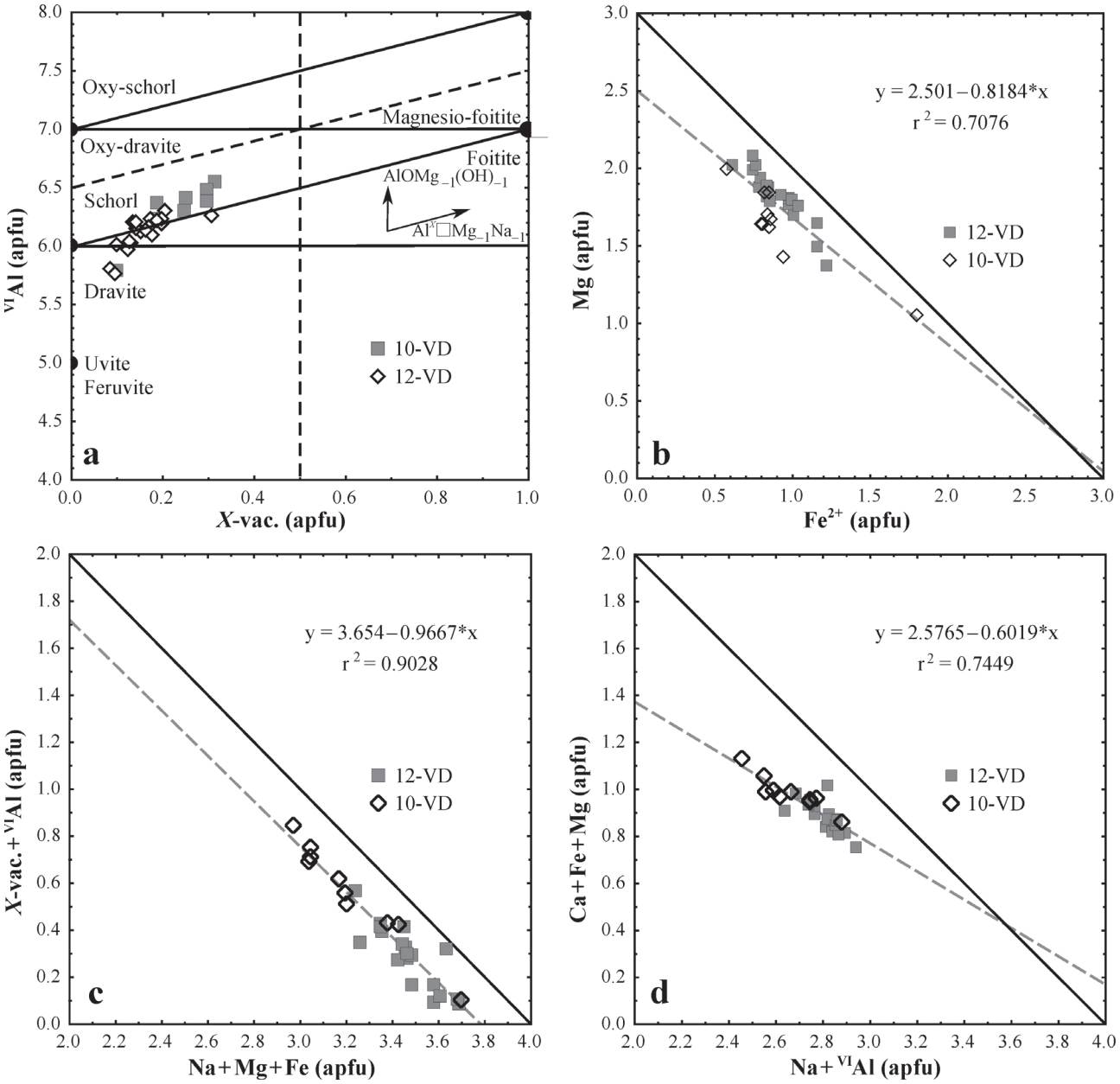

Fig. 7. Diagrams determining substitution trends in the tourmalines (n = 29) from the sandstones. Solid black lines represent an ideal trend of substitution, while dashed grey lines represent an actual trend of substitution. **a** — *X*-site vacancy vs. octahedral Al diagram with substitution vectors (Bačík et al. 2008), **b** — $MgFe^{2+}_{-1}$ substitution, **c** — $^{X}\square AlNa_{-1}(Mg, Fe^{2+})_{-1}$ substitution, **d** — $NaAlCa_{-1}(Mg, Fe^{2+})_{-1}$ substitution.

Among minor elements, the tourmalines studied are slightly enriched in Ti attaining 1.2 wt. %, 0.15 apfu, and Ca (up to 1.3 wt. %, 0.23 apfu) (Table 2). All other minor elements including F and Cl are negligible, typically near or below the detection limit of EMPA.

Discussion

Provenance of garnets

Garnets are common accessory minerals in various source rocks and their compositions are controlled by P/T conditions as well as the lithology and chemical composition of the parent rock, although some overlaps among garnets occurring in different rocks have been recognized (e.g. Asiedu et al. 2000). The garnets are widespread in numerous types of metamorphic rocks, but are also found in acid to intermediate volcanic rocks, granites and pegmatites, peridotites and kimberlites (e.g. Deer et al. 1997 and references therein). Further, they occur in the form of detrital grains in sediments (Suggate & Hall 2014).

Garnets with the predominant almandine end-member may crystallize under different conditions, from granitic melts to metamorphic rocks of amphibolite to granulite facies (Deer et al. 1997). Therefore, the interpretation of provenance of al-

madine garnets is difficult. However, since Fe-rich garnets develop mainly during barrowian type metamorphism, we can assume that the source rocks for detrital almandine garnets from the Malužiná Formation sandstones could have been garnet-mica schists, gneisses and/or amphibolites. But they may also have been derived from peraluminous granites, aplites and granitic pegmatites as well as from volcanic rocks.

Significant amounts of spessartine molecule may occur in almandine garnets from felsic igneous rocks and from metamorphic rocks, especially those in thermal aureoles (e.g.

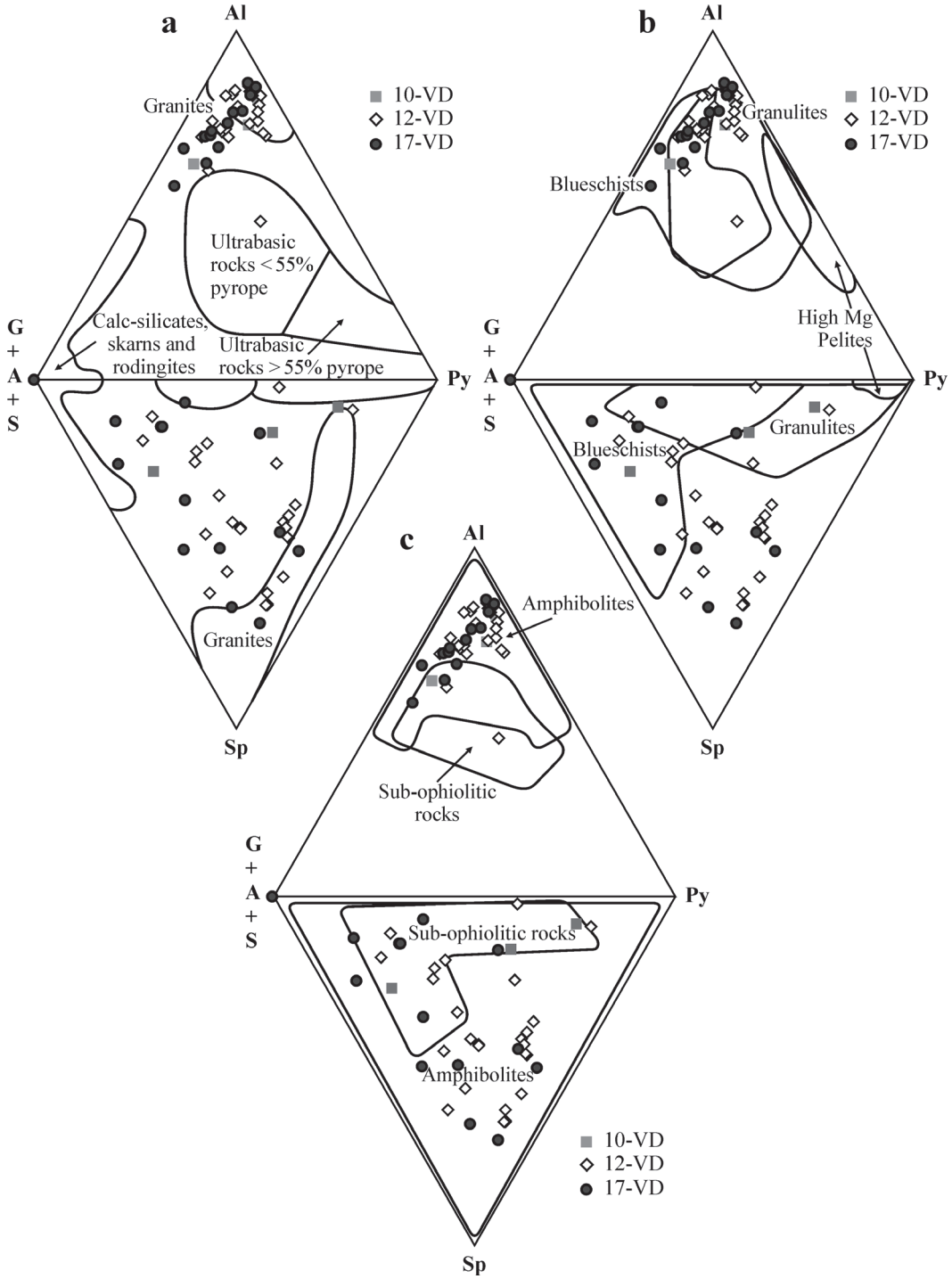

Fig. 8. Garnets ($n = 45$) from the Malužiná Formation sandstones plotted on the ternary diagrams using end-members grossular (G) + andradite (A) + schorlomite (S), almandine (Al), pyrope (Py), and spessartine (Sp), showing sub-areas characteristic of garnets with different protoliths (Suggate & Hall 2014). **a** — Ultrabasic rocks (peridotites, eclogites, and kimberlites); granites; and calc-silicates, skarns, and rodingites, 95 % of all ultrabasic garnets have pyrope >55 %, **b** — Granulites, granulite facies high-Mg pelites, and blueschists, **c** — Amphibolites and metabasic sub-ophiolitic rocks.

Deer et al. 1997). In metamorphic rocks, spessartine-rich almandine garnets are known to originate from low-grade regionally metamorphosed rocks such as metapelites, metacherts, and blue schists (Takeuchi et al. 2008). The spessartine-rich almandine garnets from the Malužiná Formation sandstones were presumably derived from metamorphic rocks, but eventually also from leucogranites or pegmatites. The above-mentioned metapelites, metacherts, and blue schists as well as leucogranites and pegmatites may be good candidates for source rocks of these spessartine-rich almandine garnets. Consequently, the origin of detrital spessartine-rich almandine garnets could be presumably derived from low-P/T metamorphic rocks such as contact-metamorphic rocks and felsic igneous rocks.

Complete grossular-almandine solid solution occurs at high pressure (Hariya & Nakano 1972; Takeuchi et al. 2008). Grossular-rich almandine garnet actually occurs in high-P/T crystalline schists (Tsujimori et al. 2000; Takeuchi et al. 2008). In this regard, the grossular-rich almandine garnets from the Malužiná Formation sandstones are considered to have been derived from high-P/T metamorphic rocks.

For garnets forming under high-grade metamorphic conditions an increase of the pyrope end-member is characteristic (Miyashiro 1953, 1973; Sturt 1962; Nandi 1967; Miyashiro & Shido 1973; Oszczypko & Salata 2005). Therefore, high-pyrope content almandine garnets occur in epidote-amphibolite to granulite facies gneisses (Miyashiro 1953; Coleman et al. 1965; Takeuchi et al. 2008). Hence, the detrital pyrope-rich almandine garnets of the Malužiná Formation sandstones may have been derived from schists and gneisses resulting from the regional metamorphism of argillaceous sediments. On the other hand, garnet peridotites and associated eclogites can be excluded as possible source rocks due to the low (<50 %) pyrope component in the studied pyrope-rich almandine garnets (Coleman et al. 1965; Deer et al. 1992; von Eynatten & Gaupp 1999).

Andradite garnet typically occurs mainly in contact or thermally metamorphosed impure calcareous sediments. Moreover, the higher oxidation state of skarns, alpine serpentinites, and some alkaline igneous rocks produces andradite-rich garnets (Deer et al. 1997; Takeuchi et al. 2008). Thus, detrital andradite garnets from the Malužiná Formation sandstones might have been derived from such thermally metamorphosed impure calcareous and/or skarn-like rocks.

Suggate & Hall (2014) discussed a large garnet compositional database compiled from the literature and showed how useful such data could be in identifying the provenance of detrital garnets. These authors calculated the six principal garnet end-member compositions (pyrope, almandine, spessartine, uvarovite, grossular, and andradite), devised a multistage methodology to match garnet compositions to source rocks, and identified a series of garnet provenance fields on ternary plots. Using Suggate & Hall's approach, we found out that the detrital garnets from the Malužiná Formation sandstones were very likely derived from amphibolites and metabasic sub-ophiolitic rocks, but derivation from granulites, blueschists, and granites cannot be excluded. Two garnet grains with andradite composition can be related to calc-silicates, skarns, and rodingites (Fig. 8).

According to the discussion above, the garnets analysed may have been derived from a variety of rock types. The additional petrographic and geochemical information available for the Malužiná Formation sandstones (Vozárová & Vozár 1988; Vďačný 2013; Vďačný et al. 2013), does not enable us to unambiguously exclude any of the aforementioned rock types as sources of the garnets.

Provenance of tourmalines

Tourmalines are the most usual B-bearing minerals in the Earth's crust. However, they accumulate in B-enriched rocks such as felsic intrusive rocks with average contents of 10 to 30 ppm B but attaining over 500 ppm in fertile granites and pegmatites (e.g. Černý 1991). The most boron enriched S-type granites are typically produced during anatectic processes in continental collision zones (London et al. 1996). Occurrences of B-enriched peraluminous magma derived from metasedimentary protolith in the back-arc volcanic environment are far rarer (Pichavant et al. 1988).

Tourmalines are present in various environments in granitic bodies — from apical parts to dispersed tourmaline inside the host rock or alternatively in breccias and veins in the granitic body (London et al. 1996). Tourmaline in apical parts usually forms thin to skeletal crystals and frequently intergrowths with quartz. It displays rapid internal chemical fractionation from schorl-dravitic core with fine oscillatory zoning to Fe-enriched alkali-deficient composition with lacking chemical zoning in the rim (London et al. 1996). In contrast, mixing processes during the Fe-Mg infiltration from the wall rock to the B-enriched magma can also result in tourmaline crystallization (Taylor et al. 1979). Tourmaline dispersed in the granitic body forms euhedral to anhedral crystals without chemical zoning and is usually Al-enriched charge-balanced by increased *X*-site vacancy or deprotonization of OH (London et al. 1996).

Tourmaline is also an abundant mineral of granitic pegmatites. These are the dominant genetic environment of Li-bearing tourmalines including elbaite and fluor-elbaite (e.g. Jolliff et al. 1986; Selway et al. 1999; Tindle et al. 2002), rossmanite (Selway et al. 1999), and liddicoatite (Teerstra et al. 1999). However, granitic pegmatites usually comprise schorlitic to foititic (Novák et al. 1999; Selway et al. 1999; Bačík et al. 2011) and more rarely also dravitic tourmalines (Novák et al. 1999, 2011; Bačík et al. 2012).

Tourmaline is also the most common B-bearing mineral in metamorphic processes as well. It is a chemically and structurally resistant mineral stable in variable P/T conditions from diagenetic environment to granulite facies (Henry & Dutrow 1996). The lower limits of its stability can be derived from its presence in the diagenetic zone of sedimentary basins and in near-surface hydrothermal deposits as low as, or lower than, 150 °C and 100 MPa (Henry et al. 1999; Moore et al. 2004). The upper thermal stability of tourmaline has been studied experimentally and also on natural samples. It is controlled by the incongruent melting of tourmaline, which has been observed in experiments between 725 and 950 °C depending on pressure and composition (e.g. Morgan & London 1989; Holtz & Johannes 1991; Wolf & London

1997; von Goerne et al. 1999; Bačík et al. 2011; London 2011; van Hinsberg 2011). Pressure stability of tourmaline is also very wide. Experimental data reveal that Mg end-member tourmaline is stable up to at least 6 GPa (Krosse 1995). Further evidence for UHP tourmalines comes from inclusions of coesite in tourmaline grains from the Kokchetav Massif in northern Kazakhstan, the Erzgebirge in Germany, and Lago di Cignano and the Dora Maira Massif in the Alps (Schertl et al. 1991; Marschall et al. 2009; Ertl et al. 2010).

Tourmaline reflects changes in P/T conditions but also in chemical composition of the host rock and associated minerals as well. It is also resistant to re-equilibration and homogenization to extreme conditions. Negligible rates of diffusion for major and trace elements in its structure were indicated by detrital compositions and sharp compositional and isotopic breaks that have persisted during prolonged periods at elevated temperature (e.g. van Hinsberg & Marschall 2007; van Hinsberg & Schumacher 2007).

Tourmaline extremely fractionates specific chemical elements (Henry & Dutrow 1996). In the medium grade it has the highest Mg/Fe and Na/Ca ratio among all phases. Similarly high Mg/Fe and Na/Ca ratios were documented in high-grade metamorphic rocks (Henry & Guidotti 1985). These fractionation trends should be considered in determination of tourmaline host-rock genetic types in metamorphic conditions.

Determination of the chemical composition of detrital tourmaline allows an estimation of its most possible genetic environment. The proportion of major elements including Al, Fe, Mg, and Ca, which are the most influenced by variable genetic environment, can be used for that purpose. Comparing proportions of Al, Fe, and Mg to empirically determined fields of various genetic types (Fig. 9a) (Henry & Guidotti 1985), the tourmalines studied can be ascribed to origin from metapelites and metapsammites coexisting (10-VD) or not coexisting (12-VD) with an Al-saturating phase. A similar observation was made on the comparison of the Ca, Fe, and Mg proportions (Fig. 9b) (Henry & Guidotti 1985). The relatively low proportion of Ca and *X*-site vacancy in the tourmalines studied suggests a medium grade of metamorphism according to Henry & Dutrow (1996)

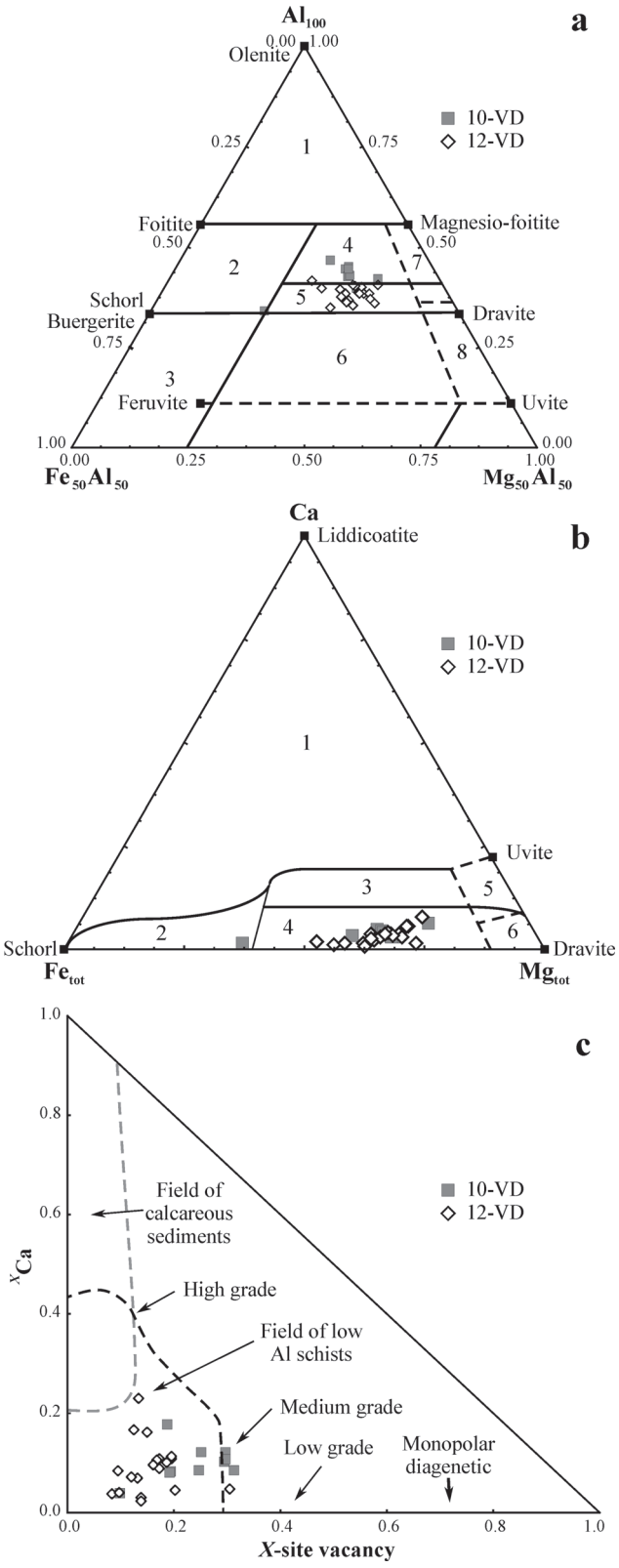

Fig. 9. Diagrams for determination of tourmaline genetic environment. Tourmalines ($n = 29$) from the sandstone samples 10-VD and 12-VD are compared with published data (fields). **a** — Al–Fe_{total}–Mg diagram (in molecular proportions). This diagram is divided into regions that define the compositional range of tourmalines from different rock types. The rock types represented are: 1 — Li-rich granitoid pegmatites and aplites, 2 — Li-poor granitoids and their associated pegmatites and aplites, 3 — Fe^{3+}-rich quartz-tourmaline rocks (hydrothermally altered granites), 4 — metapelites and metapsammites coexisting with an Al-saturating phase, 5 — metapelites and metapsammites not coexisting with an Al-saturating phase, 6 — Fe^{3+}-rich quartz-tourmaline rocks, calc-silicate rocks, and metapelites, 7 — low-Ca metaultramafics and Cr, V-rich metasediments, 8 — metacarbonates and meta-pyroxenites (modified after Henry & Guidotti 1985). **b** — Ca–Fe_{total}–Mg diagram (molecular proportions). The rock types defined by the fields in this diagram are somewhat different than those in Al–Fe_{total}–Mg diagram. These fields are: 1 — Li-rich granitoid pegmatites and aplites, 2 — Li-poor granitoids and associated pegmatites and aplites, 3 — Ca-rich metapelites, metapsammites, and calc-silicate rocks, 4 — Ca-poor metapelites, metapsammites, and quartz-tourmaline rocks, 5 — metacarbonates, 6 — metaultramafics (Henry & Guidotti 1985). **c** — Ca vs. *X*-site vacancy diagram with the fields for selected metamorphic grades and genetic types (Henry & Dutrow 1996).

(Fig. 9c). This is also supported by the relatively high Mg/Fe (1.11–3.43) and Na/Ca (2.76–38.05) ratio in most of the tourmalines studied, which is typical for the medium grade (Henry & Guidotti 1985). The possibility of high-grade metamorphic origin for the tourmalines studied is limited by the very low F content (Grew et al. 1990) and the Si content sufficient for full or almost full *T*-site occupancy, which eventually limits access of the tetrahedral Al (Grew et al. 1990; Cempírek et al. 2006) or B (Ertl et al. 2008) typical for high-grade environments. Only one tourmaline grain with a distinctly lower Mg/Fe ratio of 0.70 could be related to the Li-poor granitic genetic environment (Fig. 9a,b) (Henry & Guidotti 1985). We speculate that the subtle difference in the composition of the 10-VD and 12-VD sample could result from the slightly higher temperature during crystallization of 12-VD tourmalines or eventually from differences in the protolith composition.

Absence of inherited cores and overgrowths in the tourmalines studied suggests that these crystallized during only one genetic event. The possibility of a homogenization process can be excluded since these tourmalines do not exhibit any features (increased F, ^{T}Al, ^{T}B, and Ca content, for example) typical for high-grade metamorphism with temperatures over 700 °C necessary for initiation of diffusion in tourmalines (Bačík et al. 2011; Ertl et al. 2012).

Source areas of the Malužiná Formation sandstones and paleogeography

Previous petrographic, cathodoluminescence, and whole-rock geochemical studies on sandstones from the Malužiná Formation suggested their derivation from multiple source areas (Vďačný 2013; Vďačný et al. 2013). In these works, we speculated that the source areas were probably located quite close to the site of deposition and had broken high relief. The detritus of the Malužiná Formation sandstones was very likely stripped rapidly from the elevated areas and transported a short-distance into the sedimentary basin. Acid (felsic) plutonic rocks and low- to high-grade metamorphic rocks, felsic and mafic volcanic rocks were identified as major source lithologies. These rather broad compositional types of source rocks could be refined here to specific source-rock types by the aid of mineral chemistry of garnets and tourmalines. The present evaluation of chemical composition of these two heavy minerals revealed the following possible parent source rocks for the Malužiná Formation sandstones: (1) low-grade regionally metamorphosed rocks (metacherts, blue schists, metapelites and metapsammites coexisting or not coexisting with an Al-saturating phase), (2) thermally metamorphosed impure calcareous rocks with skarn deposits and rodingites, (3) garnet-mica schists, gneisses resulting from the regional metamorphism of argillaceous sediments, (4) amphibolites and metabasic sub-ophiolitic rocks, (5) granulites, (6) Li-poor granites and their associated pegmatites and aplites as well as (7) rhyolites. Moreover, additions from the synsedimentary andesite-basalt continental tholeiites (Vozár 1997; Dostal et al. 2003) are apparent from the presence of fragments of these rocks in the particle composition of the Malužiná Formation sandstones (Vďačný 2013; Vďačný et al. 2013).

As mentioned above, it is evident that metamorphosed and acid volcanic rocks are one of the principal sources. Several low-grade metamorphosed complexes, that mostly emerge in the form of tectonically restricted slices on the middle- and higher metamorphosed complexes or that lie directly on granitoids, occur in the pre-Pennsylvanian crystalline basement of the Central Western Carpathians (Biely et al. 1996). Acid volcanism products were found in the Northern Veporicum Unit, namely in the Jánov Grúň Complex in the Kráľovohoľské Tatry Mts (Bajaník et al. 1979; Miko 1981) and in the Krakľová Formation (Korikovskij & Miko 1992). We suppose that clastic garnets and tourmalines of the Malužiná Formation sandstones could have originated in these regions. Some of the detrital garnets and tourmalines were derived from the plutonic complexes associated with the Variscan subduction processes.

In this manner, the mineral chemistry of detrital garnets and tourmalines permitted us to more precisely interpret the character of the original basement rocks. Thus, we can now infer that the Malužiná rift system originated on a medium- to high-grade crystalline core complex composed of garnet-mica schists, gneisses, amphibolites and metabasic sub-ophiolitic rocks, and granulites penetrated with Li-poor granites, pegmatites, and aplites. This is characteristic for the Variscan terranes of the Central Western Carpathians (Biely et al. 1996; Vozárová et al. 2009). The occurrences of continental tholeiites determine the axial part of the former rift-trough. Fragments from low-grade metasediments such as metacherts, blue schists, metapelites and metapsammites, could have come from the Variscan orogenic zone.

Dostal et al. (2003) provided a tectonic reconstruction concerning the Malužiná Formation. These authors stated that the Malužiná Formation represents a part of a post-Variscan overstep suite that was formed after accretion of the Gothic terranes to Laurussia. Our previous and present findings about the provenance of the Malužiná Formation sandstones are in good agreement with their paleogeographical reconstruction that came from the studies of Tait et al. (2000) and Stampfli et al. (2001a,b, 2002). Specifically, it was assumed that the Gothic terranes, which included Armorica and correlatives, rifted off the northern Gondwanan margin in the Late Silurian, and this led to the development of the Paleo-Tethys Ocean. Subduction of the Rheic Ocean beneath the leading edge of the Gothic terranes eventually caused a collision with the southern margin of Laurussia in the Late Devonian to Early Carboniferous. Subduction of Paleo-Tethys beneath the southern margin of the accreted Gothic terranes and dextral transpressional and transtensional displacement of terranes followed in the Carboniferous and Permian. Some rift basins were converted into oceanic back-arc basins as a consequence of Triassic roll-back of the trench.

Conclusions

The chemical composition shows that almandine, spessartine-rich almandine, grossular-rich almandine, pyrope-rich almandine, and andradite garnets occur in the Permian sandstones from the Malužiná Formation in the Malé Karpaty

Mts. Tourmalines from the sandstones studied belong to a group of alkali tourmalines with dravitic composition, with the exception of a single tourmaline grain that has schorlitic composition.

The detrital garnets from the Malužiná Formation sandstones were very likely derived from garnet-mica schists, gneisses, metapelites, metacherts, amphibolites and metabasic sub-ophiolitic rocks. Derivation from granulites, blueschists, granites and volcanic rocks cannot be excluded. Some garnet grains with andradite composition can be linked with calc-silicates, skarns, and rodingites.

The tourmalines from the Malužiná Formation sandstones presumably crystallized in Al-poor as well as in Al-rich metasedimentary rocks and a minority of them also in Li-poor granitic rocks or pegmatites. Additionally, the relatively low proportion of Ca and *X*-site vacancy in the tourmalines studied suggests a medium grade of metamorphism. Absence of inherited cores and overgrowths in the tourmalines examined suggests crystallization during only one genetic event.

Judging from the chemical composition of the detrital garnets and tourmalines, the Malužiná rift system very likely originated on a medium- to high-grade crystalline core complex composed of garnet-mica schists, gneisses, amphibolites and metabasic sub-ophiolitic rocks, and granulites penetrated with Li-poor granites, pegmatites, and aplites. Fragments from low-grade metasediments such as metacherts, blue schists, metapelites and metapsammites, could have come from the Variscan Orogenic Zone.

Acknowledgments: This work was supported by the Operational Programme Research and Development through the project: Centre of Excellence for Integrated Research into the Earth's Geosphere (ITMS: 26220120064), which is co-financed through the European Regional Development Fund. This work was also supported by the Slovak Research and Development Agency under the Contract No. APVV-0546-11.

References

Asiedu D.K., Suzuki S. & Shibata T. 2000: Provenance of sandstones from the Wakino Subgroup of the Lower Cretaceous Kanmon Group, northern Kyushu, Japan. *Island Arc* 9, 1, 128–144.

Bačík P., Uher P., Sýkora M. & Lipka J. 2008: Low-Al tourmalines of the schorl-dravite – povondraite series in redeposited tourmalinites from the Western Carpathians, Slovakia. *Canad. Mineralogist* 46, 1117–1129.

Bačík P., Ozdín D., Miglierini B., Kardošová P., Pentrák M. & Haloda J. 2011: Crystallochemical effects of heat treatment on Fe-dominant tourmalines from Dolní Bory (Czech Republic) and Vlachovo (Slovakia). *Phys. Chem. Min.* 38, 599–611.

Bačík P., Uher P., Ertl A., Jonsson E., Nysten P., Kanický V. & Vaculovič T. 2012: Zoned REE-enriched dravite from a granitic pegmatite in Forshammar, Bergslagen province, Sweden: An EMPA, XRD and LA-ICP-MS study. *Canad. Mineral.* 50, 825–841.

Bajaník Š., Biely A., Miko O. & Planderová E. 1979: About Paleozoic volcanic-sedimentary Predná Hoľa Complex (Nízke Tatry Mts.). *Geol. Práce, Spr.* 73, 7–28 (in Slovak).

Biely A. (Ed.), Bezák V., Elečko M., Gross P., Kaličiak M., Konečný V., Lexa J., Mello J., Nemčok J., Potfaj M., Rakús M., Vass D., Vozár J. & Vozárová A. 1996: Explanations to the geological map of Slovakia 1:500,000. *D. Štúr Inst. Geol.*, Bratislava, 1–77 (in Slovak).

Cawood P.A. 1991: Nature and record of igneous activity in the Tonga arc, SW Pacific, deduced from the phase chemistry of derived detrital grains. In: Morton A.C., Todd S.P. & Haughton P.D.W. (Eds.): Developments in sedimentary provenance. *Geol. Soc., Spec. Publ.* 57, 305–321.

Cempírek J., Novák M., Ertl A., Hughes J.M., Rossman G.R. & Dyar M.D. 2006: Fe-bearing olenite with tetrahedrally coordinated Al from an abyssal pegmatite of the Bohemian massif at Kutná Hora: structure, crystal chemistry, and optical spectra. *Canad. Mineralogist* 44, 23–30.

Coleman R.G., Lee D.E., Beatty L.B. & Brannock W.W. 1965: Eclogites and eclogites: their differences and similarities. *Geol. Soc. Amer. Bull.* 76, 483–508.

Černý P. 1991: Fertile granites of Precambrian rare-element pegmatite fields: is geochemistry controlled by tectonic setting or source lithologies? *Precambrian Res.* 51, 429–468.

Deer W.A., Howie R.A. & Zussman J. 1992: An introduction to the rock-forming minerals. 2nd edn. *Longmans*, Essex, 1–696.

Deer W.A., Howie R.A. & Zussman J. 1997: Rock-forming minerals. Volume 1A. Orthosilicates. 2nd edn. *Longmans*, London, 1–919.

Dostal J., Vozár J., Keppie J.D. & Hovorka D. 2003: Permian volcanism in the Central Western Carpathians (Slovakia): Basin-and-Range type rifting in the southern Laurussian margin. *Int. J. Earth Sci. (Geol. Rundsch.)* 92, 27–35.

Drnzík E. 1969: Ore mineralization of Copper Bearing Permian Sandstones type of Melaphyre Series on the North-eastern Slopes of the Nízke Tatry (Low Tatras). *Miner. Slovaca* 1, 1, 7–38 (in Slovak with English summary).

Ertl A., Tillmanns E., Ntaflos T., Francis C.A., Giester G., Körner W., Hughes J.M., Lengauer C.L. & Prem M. 2008: Tetrahedrally coordinated boron in Al-rich tourmaline and its relationship to the pressure–temperature conditions of formation. *Eur. J. Mineral.* 20, 881–888.

Ertl A., Marschall H.R., Giester G., Henry D.J., Schertl H.-P., Ntaflos T., Luvizotto G.L., Nasdala L. & Tillmanns E. 2010: Metamorphic ultrahigh-pressure tourmaline: structure, chemistry, and correlation to P-T conditions. *Amer. Mineralogist* 95, 1–10.

Ertl A., Kolitsch U., Dyar M.D., Hughes J.M., Rossman G.R., Pieczka A., Henry D.J., Pezzotta F., Prowatke S., Lengauer C.L., Körner W., Brandstätter F., Francis C.A., Prem M. & Tillmanns E. 2012: Limitations of Fe^{2+} and Mn^{2+} site occupancy in tourmaline: evidence from Fe^{2+}- and Mn^{2+}-rich tourmaline. *Amer. Mineralogist* 97, 1402–1416.

Grew E.S., Chernosky J.V., Werding G., Abraham K., Marquez N. & Hinthorne J.R. 1990: Chemistry of kornerupine and associated minerals, a wet chemical, ion microprobe, and X-ray study emphasizing Li, Be, B and F contents. *J. Petrology* 31, 1025–1070.

Hariya Y. & Nakano S. 1972: Experimental study of the solid solution between the grossular-almandine series. *J. Fac. Sci. Hokkaido Univ.* 15, 173–178.

Hawthorne F.C. & Henry D.J. 1999: Classification of the minerals of the tourmaline group. *Eur. J. Mineral.* 11, 201–215.

Henry D.J. & Dutrow B.L. 1992: Tourmaline in a low grade clastic metasedimentary rock; an example of the petrogenetic potential of tourmaline. *Contr. Mineral. Petrology* 112, 203–218.

Henry D.J. & Dutrow B.L. 1996: Metamorphic tourmaline and its petrologic applications. In: Grew E.S. & Anovitz L.M. (Eds.): Boron: mineralogy, petrology and geochemistry. *Rev. in Mineralogy* 33, 503–557.

Henry D.J. & Guidotti C.V. 1985: Tourmaline as a petrogenetic indi-

cator mineral: an example from the staurolite-grade metapelites of NW Maine. *Amer. Mineralogist* 70, 1–15.

Henry D.J., Kirkland B.L. & Kirkland D.W. 1999: Sector-zoned tourmaline from the cap rock of a salt dome. *Eur. J. Mineral.* 11, 263–280.

Henry D.J., Novák M., Hawthorne F.C., Ertl A., Dutrow B.L., Uher P. & Pezzotta F. 2011: Nomenclature of the tourmaline-supergroup minerals. *Amer. Mineralogist* 96, 895–913.

Holtz F. & Johannes W. 1991: Effect of tourmaline on melt fraction and composition of first melts in quartzofeldspathic gneiss. *Eur. J. Mineral.* 3, 527–536.

Hubert J.F. 1962: A zircon-tourmaline-rutile maturity index and the interdependence of the composition of heavy mineral assemblages with the gross composition and texture of sandstones. *J. Sed. Petrology* 32, 3, 440–450.

Jian X., Guan P., Zhang D.-W., Zhang W., Feng F., Liu R.-J. & Lin S.-D. 2013: Provenance of Tertiary sandstone in the northern Qaidam basin, northeastern Tibetan Plateau: Integration of framework petrography, heavy mineral analysis and mineral chemistry. *Sed. Geol.* 290, 109–125.

Jolliff B.L., Papike J.J. & Shearer C.K. 1986: Tourmaline as a recorder of pegmatite evolution: Bob Ingersoll pegmatite, Black Hills, South Dakota. *Amer. Mineralogist* 71, 472–500.

Korikovskij S.P. & Miko O. 1992: Low-grade metasediments of the Krakľová Formation of Veporic crystalline complex. *Miner. Slovaca* 24, 381–391 (in Slovak).

Krosse S. 1995: Hochdrucksynthese, Stabilität und Eigenschaften der Borsilikate Dravit und Kornerupin sowie Darstellung und Stabilitätsverhalten eines neuen Mg-Al-Borates. *Unpubl. Ph.D. Thesis*, *Ruhr-Universität*, Bochum, 1–131.

London D. 2011: Experimental synthesis and stability of tourmaline: a historical perspective. *Canad. Mineralogist* 49, 117–136.

London D., Morgan G.B. VI & Wolf M.B. 1996: Boron in granitic rocks and their contact aureoles. In: Grew E.S. & Anovitz L.M. (Eds.): Boron: mineralogy, petrology and geochemistry. *Rev. Mineralogist* 33, 299–330.

Mange M.A. & Maurer H.F.W. 1992: Heavy minerals in colour. *Chapman & Hall*, London, 1–147.

Mange M.A. & Morton A.C. 2007: Geochemistry of heavy minerals. In: Mange M.A. & Wright D.T. (Eds.): Heavy minerals in use. *Developments in Sedimentology* 58, 345–391.

Marschall H.R., Meyer C., Wunder B., Ludwig T. & Heinrich W. 2009: Experimental boron-isotope fractionation between tourmaline and fluid: confirmation from in-situ analyses by secondary-ion mass spectrometry and from Rayleigh fractionation modelling. *Contr. Mineral. Petrology* 158, 675–681.

Miko O. 1981: Middle Paleozoic volcanic-sedimentary Jánov Grúň Formation in the Veporic crystalline of the Nízke Tatry Mts. *Geol. Zbor. Geol. Carpath.* 32, 465–474 (in Russian).

Miyashiro A. 1953: Calcium-poor garnet in relation to metamorphism. *Geochim. Cosmochim. Acta* 4, 179–208.

Miyashiro A. 1973: Metamorphism and metamorphic belts. *George Allen & Unwin Limited*, London, 1–492.

Miyashiro A. & Shido F. 1973: Progressive compositional change of garnet in metapelite. *Lithos* 6, 13–20.

Moore J.N., Christenson B.W., Allis R.G., Browne P.R.L. & Lutz S.J. 2004: The mineralogical consequences and behavior of descending acid-sulfate waters: an example from the Karaha–Telaga Bodas geothermal system, Indonesia. *Canad. Mineralogist* 42, 1483–1499.

Morgan G.B. VI & London D. 1989: Experimental reactions of amphibolite with boron-bearing aqueous fluids at 200 MPa: implications for tourmaline stability and partial melting in mafic rocks. *Contr. Mineral. Petrology* 102, 281–297.

Morton A.C. & Hallsworth C.R. 1999: Processes controlling the composition of heavy mineral assemblages in sandstones. *Sed. Geol.* 124, 3–29.

Morton A.C. & Hallsworth C.R. 2007: Stability of detrital heavy minerals during burial diagenesis. In: Mange M.A. & Wright D.T. (Eds.): Heavy minerals in use. *Developments in Sedimentology* 58, 215–245.

Morton A.C., Hounslow M.W. & Frei D. 2013: Heavy-mineral, mineral-chemical and zircon-age constraints on the provenance of Triassic sandstones from the Devon coast, southern Britain. *Geologos* 19, 1–2, 67–85.

Morton A.C., Meinhold G., Howard J.P., Phillips R.J., Strogen D., Abutarruma Y., Elgadry M., Thusu B. & Whitham A.G. 2011: A heavy mineral study of sandstones from the eastern Murzuq Basin, Libya: Constraints on provenance and stratigraphic correlation. *J. Afr. Earth Sci.* 61, 308–330.

Nandi K. 1967: Garnets as indices of progressive regional metamorphism. *Mineral. Mag.* 36, 89–93.

Nascimento M.S., Góes A.M., Macambira M.J.B. & Brod J.A. 2007: Provenance of Albian sandstones in the São Luís–Grajaú Basin (northern Brazil) from evidence of Pb-Pb zircon ages, mineral chemistry of tourmaline and palaeocurrent data. *Sed. Geol.* 201, 21–42.

Novák M., Selway J.B., Černý P., Hawthorne F.C. & Ottolini L. 1999: Tourmaline of the elbaite-dravite series from an elbaite-subtype pegmatite at Blizna, southern Bohemia, Czech Republic. *Eur. J. Mineral.* 11, 557–568.

Novák M., Škoda R., Filip J., Macek I. & Vaculovič T. 2011: Compositional trends in tourmaline from intragranitic NYF pegmatites of the Třebíč pluton, Czech Republic: an electron microprobe, Mössbauer and LA-ICP-MS study. *Canad. Mineralogist* 49, 359–380.

Novotný L. & Badár J. 1971: Stratigraphy, sedimentalogy and mineralization in the Upper Paleozoic of the Choč Unit in the Ne Part of the Low Tatras Mts. *Miner. Slovaca* 3, 9, 23–41 (in Slovak with English summary).

Oszczypko N. & Salata D. 2005: Provenance analyses of the Late Cretaceous–Palaeocene deposits of the Magura Basin (Polish Western Carpathians) — evidence from a study of the heavy minerals. *Acta Geol. Pol.* 55, 3, 237–267.

Pichavant M., Kontak D.J., Valencia-Herrera J. & Clark A.H. 1988: The Miocene-Pliocene Macusani volcanics, SE Peru. I. Mineralogy and magmatic evolution of a two-mica aluminosilicate-bearing ignimbrite suite. *Contr. Mineral. Petrology* 100, 300–324.

Planderová E. 1973: Palinological research in the melaphyre series of the Choč Unit in the NE part of Nízke Tatry between Spišský Štiavnik and Vikartovce. *Geol. Práce, Spr.* 60, 143–168.

Planderová E. & Vozárová A. 1982: Biostratigraphical correlation of the Late Paleozoic formations in the West Carpathians. In: Sassi F.P. (Ed.): *Newsletter 4, IGCP Pr. No. 5*, Padova, 67–71.

Rojkovič I. 1997: Uranium mineralization in Slovakia. *Acta Geol. Univers. Comen., Monogr.*, Bratislava, 1–117.

Selway J.B., Novák M., Černý P. & Hawthorne F.C. 1999: Compositional evolution of tourmaline in lepidolite-subtype pegmatites. *Eur. J. Mineral.* 11, 569–584.

Schertl H.-P., Schreyer W. & Chopin C. 1991: The pyrope-coesite rocks and their country rocks at Parigi, Dora Maira Massif, western Alps: detailed petrography, mineral chemistry and PT-path. *Contr. Mineral. Petrology* 108, 1–21.

Stampfli G.M., von Raumer J.F. & Borel G.D. 2002: Paleozoic evolution of pre-Variscan terranes: From Gondwana to the Variscan collision. In: Martínez Catalán J.R., Hatcher R.D. Jr., Arenas R. & Díaz García F. (Eds.): Variscan-Appalachian dynamics: The building of the late Paleozoic basement: Boulder, Colorado. *Geol. Soc. Amer., Spec. Pap.* 364, 263–280.

Stampfli G.M., Borel G.D., Cavazza W., Mosar J. & Ziegler P.A. 2001a: Palaeotectonic and palaeogeographic evolution of the

western Tethys and Peri-Tethyan domain. *Episodes* 24, 222–228.

Stampfli G.M., Mosar J., Favre P., Pillevuit A. & Vannay J.-C. 2001b: Permo-Mesozoic evolution of the western Tethyan realm: the Neotethys/East-Mediterranean connection. In: Ziegler P.A., Cavazza W., Robertson A.H.F. & Crasquin-Soleau S. (Eds.): Peri-Tethys memoir 6: Peri-Tethyan rift/wrench basins and passive margins. *IGCP Pr. No. 369*, Paris, 51–108.

Sturt B.A. 1962: The composition of garnets from pelitic schists in relation to the grade of regional metamorphism. *J. Petrology* 3, 181–191.

Suggate S.M. & Hall R. 2014: Using detrital garnet compositions to determine provenance: a new compositional database and procedure. In: Scott R.A., Smyth H.R., Morton A.C. & Richardson N. (Eds.): Sediment provenance studies in hydrocarbon exploration and production. *Geol. Soc. London, Spec. Publ.* 386, 373–393.

Tait J., Schatz M., Bachtadse V. & Soffel H. 2000: Paleomagnetism and Paleozoic paleogeography of Gondwana and European terranes. In: Franke W., Haak V., Oncken O. & Tanner D. (Eds.): Orogenic processes: quantification and modelling in the Variscan belt. *Geol. Soc. London, Spec. Publ.* 179, 21–34.

Takeuchi M., Kawai M. & Matsuzawa N. 2008: Detrital garnet and chromian spinel chemistry of Permian clastics in the Renge area, central Japan: Implications for the paleogeography of the East Asian continental margin. *Sed. Geol.* 212, 25–39.

Taylor B.E., Foord E.E. & Friedrichsen H. 1979: Stable isotope and fluid inclusions studies of gem-bearing granitic pegmatite-aplite dikes, San Diego County, California. *Contr. Mineral. Petrology* 68, 187–205.

Teerstra D.K., Černý P. & Ottolini L. 1999: Stranger in paradise: liddicoatite from the High Grade Dike pegmatite, southeastern Manitoba, Canada. *Eur. J. Mineral.* 11, 227–235.

Tindle A.G., Breaks F.W. & Selway J.B. 2002: Tourmaline in petalite-subtype granitic pegmatites: Evidence of fractionation and contamination from the Pakeagama Lake and Separation Lake areas of northwestern Ontario, Canada. *Canad. Mineralogist* 40, 753–788.

Tsujimori T., Ishiwatari A. & Banno S. 2000: Eclogitic glaucophane schist from the Yunotani valley in Omi Town, the Renge metamorphic belt, the Inner Zone of southwestern Japan. *J. Geol. Soc. Japan* 106, 353–362 (in Japanese with English abstract).

van Hinsberg V.J. 2011: Preliminary experimental data on trace-element partitioning between tourmaline and silicate melt. *Canad. Mineralogist* 49, 153–163.

van Hinsberg V.J. & Marschall H.R. 2007: Boron isotope and light element sector zoning in tourmaline: implications for the formation of B-isotopic signatures. *Chem. Geol.* 238, 141–148.

van Hinsberg V.J. & Schumacher J.C. 2007: Intersector element partitioning in tourmaline: a potentially powerful single crystal thermometer. *Contr. Mineral. Petrology* 153, 289–301.

Vďačný M. 2013: Provenance of the Malužiná Formation sandstones (Western Carpathians, Slovakia): constraints from standard petrography, cathodoluminescence imaging, and mineral chemistry of feldspars. *Geol. Quart.* 57, 1, 61–72.

Vďačný M., Vozárová A. & Vozár J. 2013: Geochemistry of the Permian sandstones from the Malužiná Formation in the Malé Karpaty Mts (Hronic Unit, Western Carpathians, Slovakia): implications for source-area weathering, provenance and tectonic setting. *Geol. Carpathica* 64, 1, 23–38.

von Eynatten H. & Gaupp R. 1999: Provenance of Cretaceous synorogenic sandstones in the Eastern Alps: constraints from framework petrography, heavy mineral analysis and mineral chemistry. *Sed. Geol.* 124, 81–111.

von Goerne G., Franz G. & Wirth R. 1999: Hydrothermal synthesis of large dravite crystals by the chamber method. *Eur. J. Mineral.* 11, 1061–1078.

Vozár J. 1977: Magmatic rocks of the tholeiite series in the Permian of the Choč nappe in the West Carpathians. *Miner. Slovaca* 9, 4, 241–258 (in Slovak with English summary).

Vozár J. 1997: Rift-related volcanism in the Permian of the Western Carpathians. In: Grecula P., Hovorka D. & Putiš M. (Eds.): Geological evolution of the Western Carpathians. *Miner. Slovaca – Monograph*, Bratislava, 225–234.

Vozárová A. & Vozár J. 1981: Lithostratigraphical subdivision of Late Paleozoic sequences in the Hronic unit. *Miner. Slovaca* 13, 5, 385–403 (in Slovak with English summary).

Vozárová A. & Vozár J. 1988: Late Paleozoic in West Carpathians. *D. Štúr Inst. Geol.*, Bratislava, 1–314.

Vozárová A., Frank W., Kráľ J. & Vozár J. 2005: $^{40}Ar/^{39}Ar$ dating of detrital mica from the Upper Paleozoic sandstones in the Western Carpathians (Slovakia). *Geol. Carpathica* 56, 6, 463–472.

Vozárová A., Ebner F., Kovács S., Kräutner H.-G., Szederkenyi T., Krstić B., Sremac J., Aljinovič D., Novak M. & Skaberne D. 2009: Late Variscan (Carboniferous to Permian) environments in the Circum Pannonian Region. *Geol. Carpathica* 60, 1, 71–104.

Wolf M.B. & London D. 1997: Boron in granitic magmas: stability of tourmaline in equilibrium with biotite and cordierite. *Contr. Mineral. Petrology* 130, 12–30.